Proceedings World Geothermal Congress 2020+1
Reykjavik, Iceland, April - October 2021

Geothermal Reservoir Characterization Using Seismic and Machine Learning - A Case Study from the Geneva Basin

L. Perozzi[1], L. Guglielmett[1]i, A. Moscariello[1]

1 Department of Earth Sciences, University of Geneva. Rue des Maraichers 13, 1205 Geneva (Switzerland)

lorenzo.perozzi@unige.ch

Keywords: Automatic fault detection, Unsupervised machine learning, Quantitative seismic analysis, Clustering, K-means

ABSTRACT

This paper focuses on the quantitative interpretation of the existing seismic lines of the Canton of Geneva in the framework of the Innosuisse funded project GECOS (Geothermal Energy Chance of Success). The goal of GECOS is to reduce the costs and the exploration risk for geothermal exploration by integrating high-resolution data acquisitions such as gravity, S-waves reflection seismic and 3D DAS VSP (Distributed Acoustic Sensing Vertical Seismic Profiling) as well as vintage seismic data. The main geological challenges in geothermal exploration in the Geneva area are the characterization of the lithological heterogeneities and the fault zones affecting potential geothermal targets in the Quaternary sediments, Tertiary Molasse sequence and the Mesozoic Units.

The subsurface risk and uncertainty quantification involve, for example, the characterization of fractures (fault), the facies interpretation and the evaluation of geomechanical parameters like brittleness, Poisson's ratio and Young's modulus from seismic data and well logs. Artificial intelligence and in particular machine learning (ML) are promising techniques which popularity is growing exponentially and have proven to be very useful for big data assimilation. In fact, standard techniques are limited to integrate few variables. However, ML algorithms perform very well with hundreds to thousands of variables. The aim of this work is to demonstrate how these quantitative techniques can be applied to fault detection, seismic facies interpretation, and to automatically identify lithofacies based on well-log measurements. Results show that these techniques are an additional tool that could help improve the knowledge and characterize a geological reservoir, thus reduce the subsurface uncertainty, if and only if they are applied together with a domain specialist such as experimented geologists and geophysicists.

1. INTRODUCTION

The increased energy demand together with the political vision of reducing the use of fossil fuels for heat production in the Canton of Geneva triggered the development of medium to long-term activities, under the umbrella of the Geothermie 2020 program (Moscariello, 2016). This program aims at exploring and ultimately implementing geothermal energy focusing first on heat production and storage, and then on power production. The program is driven by the Services Industriels de Genève (SIG), the Geological Survey of the Canton of Geneva (GESDEC) and is supported by national authorities such as the Swiss Federal Office of Energy (SFOE) and national research programs (i.e., the Swiss Competence Centre for Energy Resources, (SCEER). The exploration activities carried out since now allowed identifying potential geological targets at shallow/medium (500-3000 m) to large depth (>3000 m) depths to combine heat and power production (Moscariello *et al*., 2020).

The identification and characterization of the subsurface prior drilling is crucial to define potential geothermal targets. 2D seismic has proved to be the most effective method to image the Mesozoic formations in the Geneva Basin (Moscariello, et al., 2020). However, the data quality differs significantly from the oldest to the most recent lines.

This study aims at evaluating the added value of quantitative and ML technique to enhance information from seismic lines by offering an additional tool to better outline and characterize the Geneva Basin for geothermal energy exploration.

This paper focuses in particular on the following:

- Developing an automatic fault interpretation algorithm that can be easily applied on 2D seismic lines available on the Geneva Basin;
- Defining attributes from existing 2D seismic data that can be clustered to obtain quantitative information on geothermal seismic facies and geomechanical properties;
- Classify geophysical logs into lithofacies using unsupervised machine learning approach.

2. GEOLOGICAL SETTINGS

The Geneva Basin (GB) covers an area of about 2000 km^2 extending from the town of Nyon to the NE, down to Vuache Mountain to the SW and it is limited by the Jura Haute-Chain to the NW and by the subalpine nappes towards SE.

The GB is the westernmost part of the North Alpine Foreland Basin that extends from the Savoy region in France to Linz in Austria (Kuhlemann and Kempf, 2002). Four major lithological units are recorded at depth (Kempf and Pfiffner, 2004; Kuhlemann and Kempf, 2002; Mazurek *et al*., 2006; Moscariello *et al*., 2020): the crystalline basement including the Permo-Carboniferous troughs (Moscariello *et al*., 2014), its sedimentary cover composed respectively of Mesozoic carbonate units, Cenozoic sediments (Figure 1).

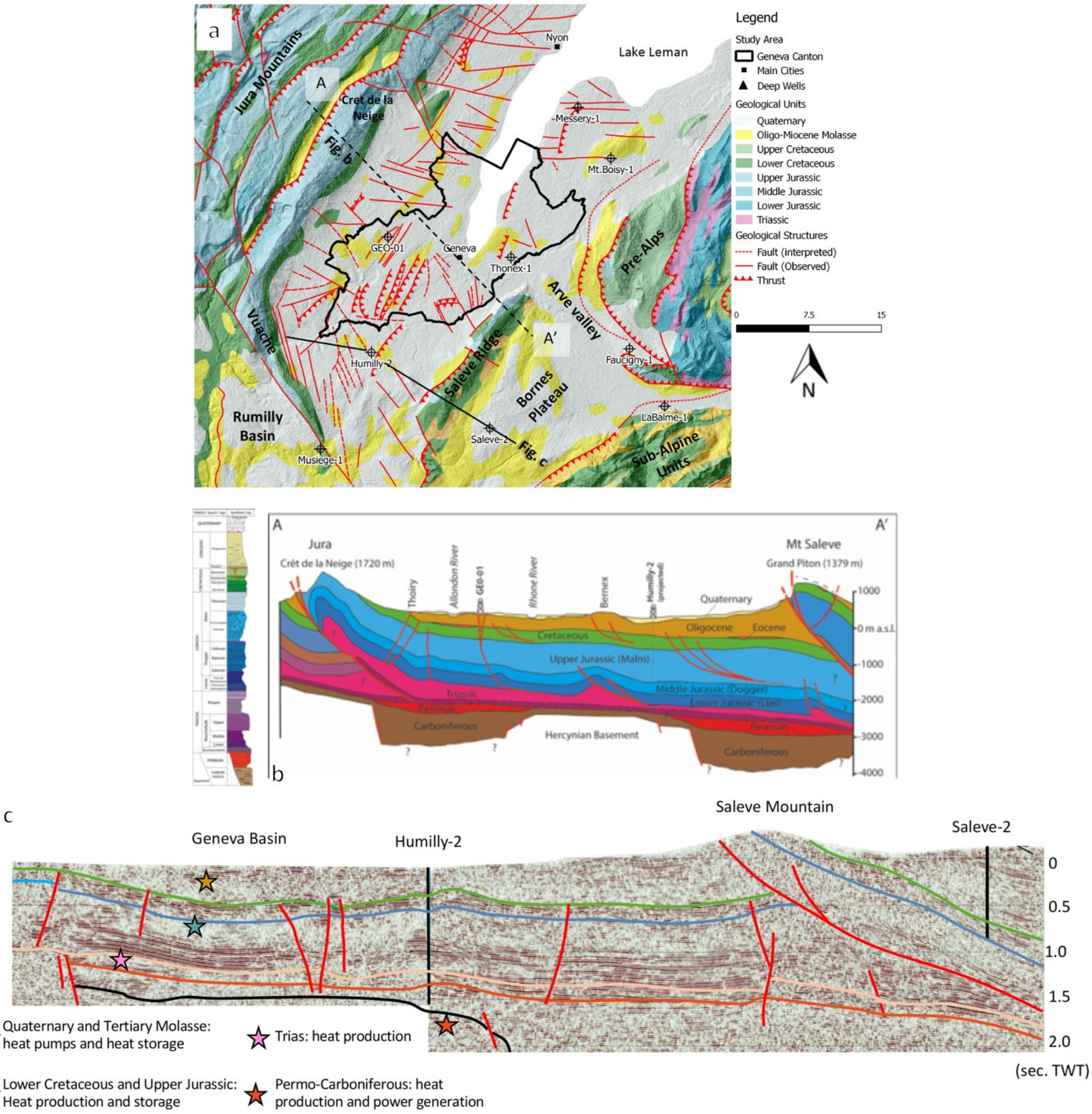

Figure 1 - a) Geological map over the Geneva Basin with indication of the main deep wells (modified. from Brentini, 2018); b) Cross section though the GB (Moscariello *et al*., 2020). c) Seismic section showing the general structural setting and the main geothermal targets (modified from Moscariello, 2016).

The tectonic evolution of the GB is associated with the alpine compressional phase that caused the decoupling of the sedimentary succession from the basement by a detachment surface occurring on the Triassic evaporites (Affolter and Gratier, 2004; Arn *et al*., 2005; Guellec *et al*., 1990; Sommaruga, 1999). Additionally, inherited basement reliefs and normal faults bounding Permo-Carboniferous troughs might have played a role in the nucleation of the Mesozoic north-westward thrusts observed in the SE sector of the Geneva Basin and Bornes Plateau (Gorin *et al*., 1993; Signer and Gorin, 1995).

In response to the alpine compression, the Mesozoic and Cenozoic sedimentary cover of the GB underwent some shortening locally coupled to a rotational motion. This shortening was absorbed through the structuration of the fold and thrust reliefs of the Jura arc mountains during the late Miocene and Early Pliocene (Affolter and Gratier, 2004; Homberg *et al.*, 2002; Meyer, 2000) and by the coeval formation of accommodation of strike-slip faults. The most relevant surface evidence of such structures is the NW-SE Vuache fault (Charollais *et al*., 2013), which crosscuts the entire basin and bounds the western side of the study area.

In the GB, apart from the regional Vuache fault, series of smaller-scale NW-SE striking left-lateral wrench faults affect the southwestern part of the Geneva area. Unlike the Vuache fault, no obvious connections between these structures and the Jura Mountain can be drawn across the study area (Brentini, 2018; Rusillon, 2018) as suggested in previous interpretations (Signer and Gorin, 1995). Towards the northeast of the basin, the structural configuration is dominated by E-W striking faults. NW-SE and E-W strike slip faults occur as a series of sub-vertical individual faults often affecting most of the Mesozoic sequence, down to the Triassic detachment surface, with associated smaller-scale sets of conjugates. Upward extension through the Cenozoic interval of the most important faults often appears as flower structures. This shallow subsurface expression is consistent with fault geometries observed in Cenozoic Molasse outcrops (Angelillo, 1983; Charollais *et al*., 2007). The maximum horizontal stress orientation in the study area shows two main trends: central and eastern part have a WNW-ESE to NW-SE S_H orientation, whereas the south-western region is controlled by a NE-SW orientation (Becker, 2000).

3. DATASET

3.1 Seismic data

About 200 km of 2D seismic lines are available over the Geneva Basin, corresponding principally to 4 acquisition campaigns undertaken from 1987 to 2015, as well as a selection of unitary lines issued from earlier acquisition campaigns (1972-1977) to complete the seismic dataset toward the Northeast of the study area (Figure 2).

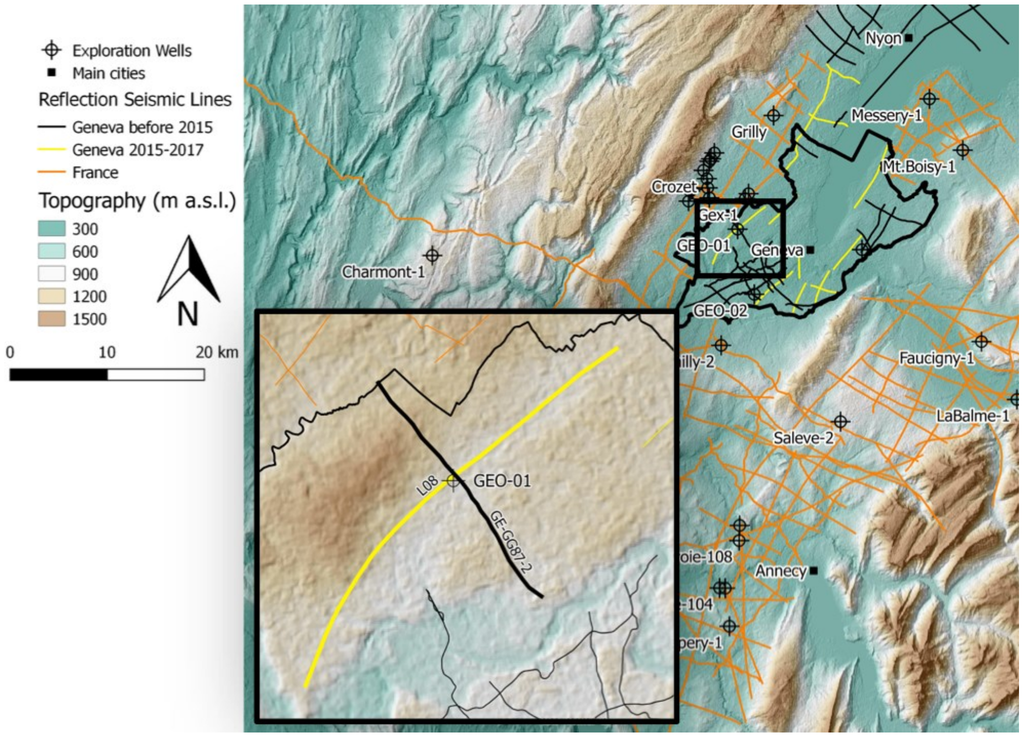

Figure 2 – Distribution of seismic line over the Geneva Basin. The bottom left zoom shows the two lines and the well-used for this study (modified from Moscariello et al., 2020).

For this study, two time-migrated, 2D seismic reflection profiles intersecting the well GEo-01 have been retained to apply the proposed methodology, highlighted in the bottom left box of the figure 2. Lines GG87-02 and SIG 2015-L08 are oriented NW-SE and NE-SW, covering approximately a distance of 4630 m and 8039 m, with a trace spacing of 15 m and 10 m respectively. Vertically, the profiles were recorded down to 4000 ms and 2000 ms respectively (Lo, 2019).

3.2 Borehole data

Geo-01 is an exploration well drilled by Services Industriels de Genève (SIG) on fall 2017. It reached a depth of 744.06 m MD, extending down to the Jurassic. Unfortunately, logging was only successful down to 533 m MD near the top Chambotte Fm (Cretaceous) due to unstable wellbore condition. Geophysical logs were available from 15 to 532 m MD at a resolution of 15 cm, including caliper, total gamma ray, spectral gamma ray (potassium, thorium and uranium), bulk density, sonic, neutron porosity, photoelectric effect, resistivity (deep and shallow), induction resistivity and spontaneous potential logs (Lo, 2019).

4. METHODOLOGY

There has been much excitement recently about big data and the need for data scientists who possess the ability to extract meaning from it. Geoscientists, meanwhile, have been doing science with voluminous data for years, without needing to brag about how big it is. But now that large, complex data sets are widely available, there has been a proliferation of tools and techniques for analyzing them. Many free and open-source packages now exist that provide powerful additions to the geoscientist's toolbox, much of which used to be only available in proprietary software platforms. One of the best examples is (Pedregosa *et al*., 2011) a collection of easy-to-use tools for data processing and machine learning in Python.

The aim of this work is to provide a quantitative methodology to enhance information from existing data and thus reduce the uncertainty during the geothermal exploration phase. To accomplish this, we propose a three-step approach including an automated fault interpretation, and an unsupervised learning technique for both seismic facies interpretation and to identify lithofacies based on well-log measurements.

4.1 Automatic fault detection using optimal surface voting

One of the key aspects to characterize a geothermal basin is to understand clearly the structural network of the seismic dataset and reducing risk in well placement. Traditionally, this task is done by an experimental geologist/geophysicist by manually picking the faults identified on seismic images, which is both a tedious and time-consuming task. Fault interpretation from a seismic image often requires first computing a fault attribute image, in which only the fault features are dominant while reflections and other features are removed. Numerous seismic attributes have been proposed to detect faults by measuring seismic reflection continuity such as semblance (Marfurt *et al*., 1998) and coherency (Marfurt *et al*., 1999, Li and Lu, 2014) or reflection discontinuity such as variance (Van Bemmel and Pepper, 2000, Randen *et al*., 2001). However, these seismic attributes can be sensitive to noise and stratigraphic features, which are also apparent as reflection discontinuities within a seismic image. The methods that have to date delivered the best results are based on the structure-oriented semblance attribute (Hale, 2013). Recently deep learning techniques have sparked a lot of interest (Wu *et al*., 2019), but they require a large amount of data to train the model.

For this work we apply a novel method, developed by Wu and Fomel (2018), to efficiently compute a new fault attribute map of voting scores from an input fault attribute image. In the first step, a new attribute called fault plane is derived from the optimized variance of the seismic image. In the second step, the extrema of the fault plane attribute are extracted through a thinning process. In this method, seed points are picked from the input attribute image and used as control points to compute optimal surface patches that pass through the control points and follow globally maximum fault attribute values. Then, all the computed surfaces are computed as voters. Voting scores are then defined for each voter by using fault attribute values that are smoothed along the surface voter. Finally, a voting score map is computed as a new fault attribute image, in which fault features (with high scores) are much cleaner, sharper, and more continuous than those in the input attribute image. For detailed information, we refer the reader to the paper of Wu and Fomel (2018).

4.2 Data-driven seismic facies interpretation

Automatic seismic facies analysis aims to classify similar seismic traces based on traditional attributes such as amplitude, similarity and energy. Beyond these traditional attributes exist a large family of metrics that are developed for image processing tasks and that can be applied to seismic data. The idea is to imitate the simple pattern recognition rules our brains intuitively and continuously apply when we look at seismic data. For example, Haralick texture (Haralick *et al*., 1973) are statistic metrics that returns textural information based on a statistical texture classification using the grey level co-occurrence matrix (GLCM), that is a measure of how often different combinations of pixel brightness values occur in an image.

For this work we propose to use an unsupervised learning algorithm, K-means (Lloyd, 1982), that allows to identify similar group of clusters (or facies) within a seismic image. The idea is to integrate traditional attributes (similarity, energy, amplitude), the Haralick texture attribute and the fault plane attribute computed in 4.1, to group similar seismic facies together and classify the seismic field into facies that have similar features. The K-means algorithm classifies the seismic data by trying to separate samples in n clusters of equal variances, where the number of clusters has to be specified.

4.3 Automatic lithology classification using geophysical logs

Classification of different lithofacies is crucial in seismic interpretation because different rocks have different permeability and fluid saturation for a given porosity but is often subject to interpretation bias as it is traditionally performed by an expert who assigns wireline log responses to a lithology, and then cross-references the interpretation to the lithology observed in cores (when available). Challenges of the manual facies interpretation are often associated with a lack of data, poor data quality, interpretation uncertainty, variation in terminological conventions, and an increase in the expert's workload with large datasets. Therefore, several alternative approaches have been proposed, including a supervised machine learning technique (Hall, 2016), where they proposed to use a small dataset of seven wireline logs and associated interpreted facies extracted from ten wells of the Hugoton gas field (Dubois *et al*., 2007) in southwest Kansas in order to predict geologic facies in two additional wells based on wireline measurements only.

Since we do not have sufficient wells and lithofacies interpretation to train a supervised algorithm, we decide to test an unsupervised algorithm with geophysical logs measurements from GEo-01 well. We then evaluate its performance to classify lithofacies and we compare the results with a lithological log (Hydro-Geo Environnement Sarl, 2018) following the drilling of the well. As for the previous section, we propose to use the K-means algorithm (Lloyd, 1982), that allows to identify similar group of clusters (or facies) within a dataset of different wireline logs measurements. For this particular case, we use 14 different geophysical logs that are presented on the figure 6a.

5. RESULTS

This section shows the results obtained by applying the two-step methodology to 2D seismic profiles GG87-02 and SIG 2015-L08. The optimal surface path voting algorithm has been adapted and applied to all traces between 0 and 1200 ms.

5.1 Automatic fault detection

5.1.1 Seismic profile GG87-02

Figure 3b shows the resulting voting score map for a probability of having a fault/fracture greater than 70%. The result is compared with a knowledge-driven interpretation (Moscariello *et al*., 2020), figure 3c. The fault structures interpreted around the well GEo-01 are reasonably well detected using the two different approaches. The faults detected automatically using the optimal surface voting approach is less continuous compared to the knowledge-driven approach. However, the results highlight a different fracture/fault system on the two sides of the well GEo-01. The left part has a lower fracture density probably corresponding to a tight formation, however, the right part shows a denser fracture system corresponding to a brittle formation.

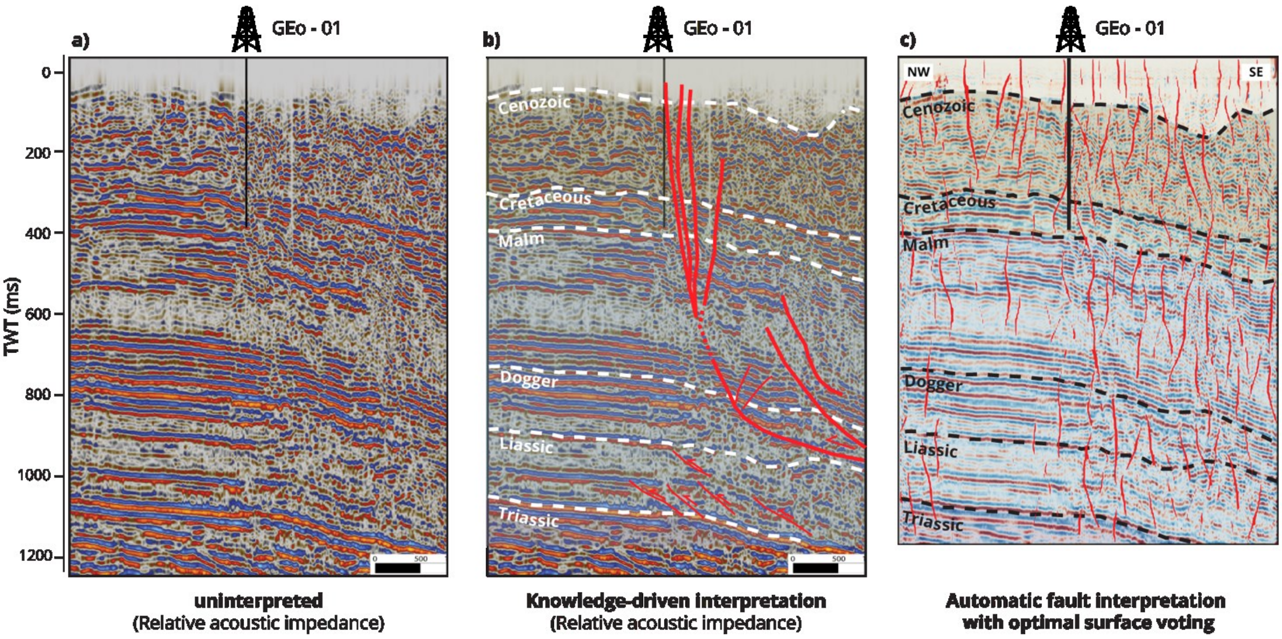

Figure 3: Seismic profile GG87-02. a) Uninterpreted and b) interpreted (Moscariello *et al*., 2020); c) Automatic fault interpretation with optimal surface voting.

5.1.1 Seismic profile SIG-2015-L08

Figure 4c shows the resulting voting score map for a probability of having a fault/fracture greater than 70% on the seismic line SIG-2015-L08. The result shows a chaotic fault system on all seismic profile. Cretaceous and Malm units seems to be slightly tighter, especially in the left side of the GEo-01 well.

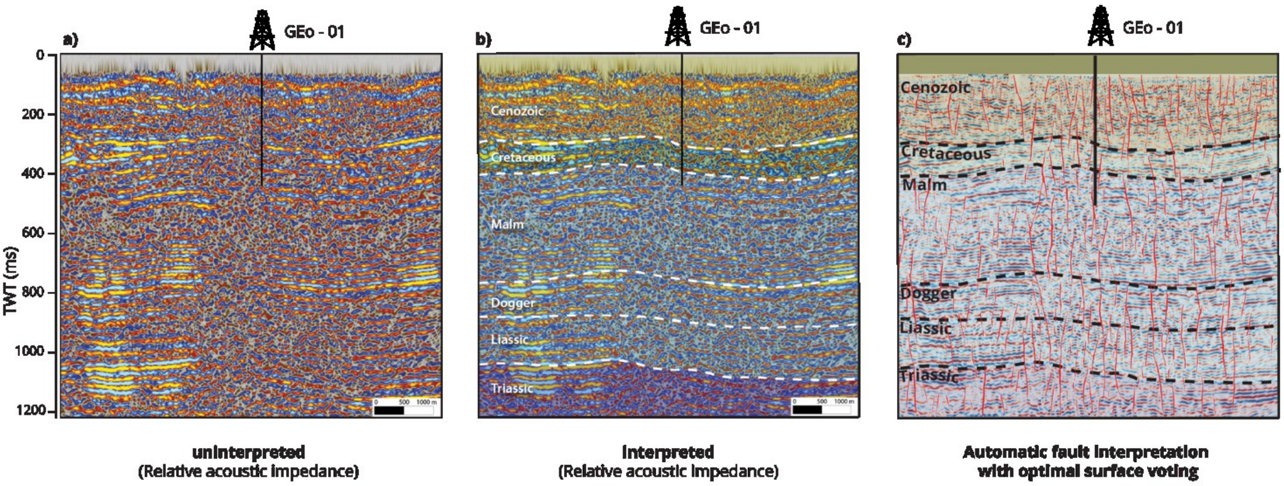

Figure 4: Seismic profile SIG-2015-L08. Uninterpreted (a) and interpreted as part of the GeoMol project (Clerc, 2016) (b). Automatic fault interpretation with optimal surface voting (c).

5.2 Seismic facies classification using K-means

The Figure 5 shows the results for the seismic line GG8702 and SIG-2015-L08, obtained by clustering seven seismic attributes: similarity, energy, amplitude, three Haralick texture statistics and the fault map attribute obtained in 5.1. The optimal number of clusters has been defined following the elbow method (Thorndike,1953) and it has been fixed to 3.

The results show a clear classification of the seismic line into three facies (yellow, pink and blue), that can be interpreted as unfractured intervals zone (yellow facies), especially visible in the left part of the GG8702 section; a likely occurrence of fractures zone (blue facies), which cover the most of the seismic line SIG-2015-L08 and a region of likely occurrence of fractures and small offset faults (pink facies), that correspond to the fault network system identified in 5.1.

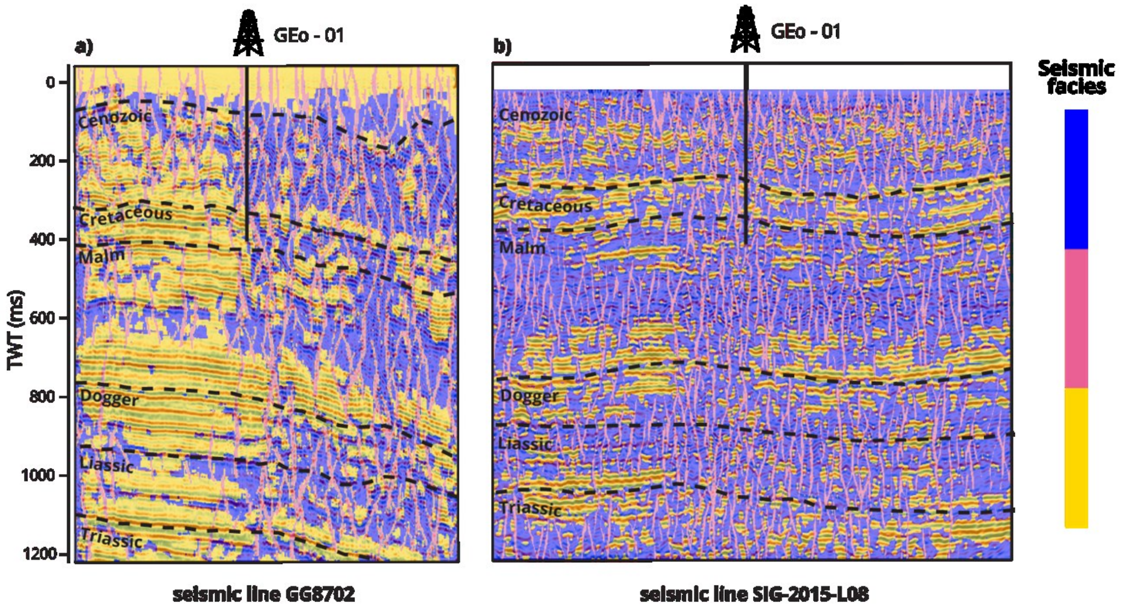

Figure 5: Seismic facies obtained by clustering seismic attributes, a) seismic line GG8702; b) seismic line SIG-2015-L08.

5.3 Lithology classification using K-means

Figure 6a shows the ~~14~~ the geophysical logs used with the proposed approach. We decided to use log measurements from 30 to 526 m, since the quality of data on the top and the bottom of the well logs are of poor quality for our purpose. Figure 6c shows the original lithology compiled by Hydro-Geo environnement, (2018). In the original litholog, 9 lithologies have been identified, however, two of them (breccia/conglomerate and shale) appeared only once in the litholog. For this reason, we decided to use the K-means algorithm with the number of clusters fixed to 7 for the lithofacies classification. The result is shown in Figure 6b, and the best result is obtained after applying a smoothing with a Gaussian kernel (Worsley *et al*., 1996). Comparing the smoothed classification with the original log, we can clearly see that there is a good fit, indicating that geophysical logs are able to capture the lithology trend in the well. However, at small scale, we can see that there are some discrepancies especially in identifying sandstone, marly sandstone and sandy marls lithologies (indicated by sable/grès, grès marneux, and marne grèseuse respectively in Figure 6c).

6. CONCLUSIONS

The Geneva Basin is considered to have a great potential for geothermal resources which developed during the complex sedimentary and tectonic history of this region. To assess this potential a sound analysis of existing data in addition to acquisition of new high-resolution data (e.g. geophysical, lithological etc) is necessary to evaluate the subsurface uncertainty (Moscariello *et al.,* 2020) and mitigate the economic risk of geothermal projects.

For this work we applied quantitative methods to automatic fault detection, seismic facies classification and lithology classification from geophysical log measurements. The aim of this work was to demonstrate how quantitative methods could be used as an added tool for interpreting seismic and well data.

First, we applied a fault detection algorithm to available seismic profile. This method provides a first quick structural evaluation of seismic data. However, the outcomes are strongly dependent on seismic quality (i.e. signal-to-noise ratio; lateral reflector continuity, etc.) which may be affected by processing artefacts and acquisition limitations (i.e., surface constrains). In addition, quality check and result validation will need to be carried out by using the general knowledge of the regional and local structural framework before those data could be used to steer static and/or dynamic geological modelling.

Second, an unsupervised clustering algorithm allowed us to integrate classical seismic attributes such as amplitude, energy and similarity with texture attributes and fault plane attributes to obtain a seismic facies image that allows us to better identify tight and brittle formations as well as faults/fractures systems.

Finally, an unsupervised classification approach allowed us to produce quickly a pseudo-litholog from geophysical logs available on GEo-01 well which could be used by an expert to guide his geological interpretation.

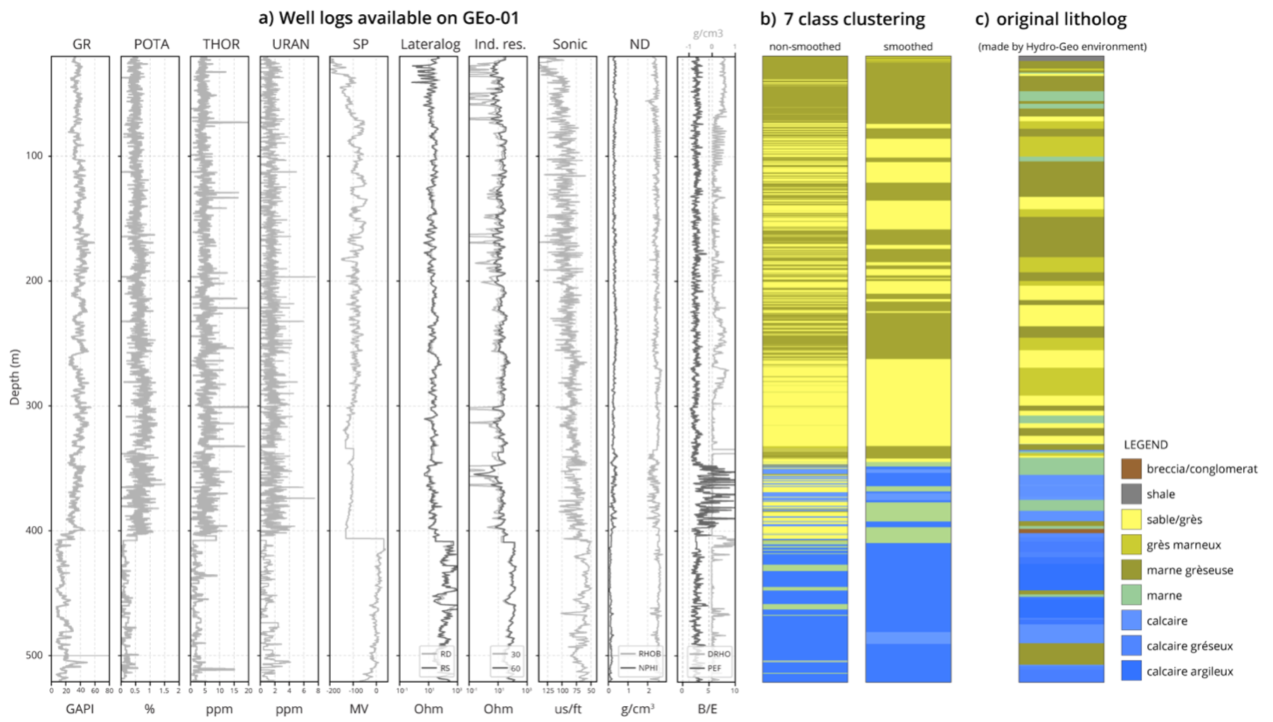

Figure 6: a) Example of geophysical logs available for the well GEo-01; b) K-means classification of lithologies using geophysical logs; c) original litholog (Geo-Hydro environnement, 2018).

AKNOWLEDGNENTS

This research described in this paper has been carried out in the framework of the Innoswiss funded program GECOS. This paper is also a contribution to the Swiss national research program SCCER SoE and the EC funded GEOTHERMICA/HEATSTORE program.

REFERENCES

Affolter, T. and Gratier, J.-P., Map view retrodeformation of an arcuate fold-and-thrust belt: The Jura case. *Journal of Geophysical Research,* (2004).109(B3).

Angelillo, V. Les Marnes et Grès gris à gypse («Molasse grise») du bassin genevois. Geneva: In Université de Geneve (Ed.), Géologie, sédimentologie, stratigraphie (1983).

Arn, R., Conrad, M. A. and Weidmann, M., Nyon. Atlas géologique de la Suisse 1:25'000, feuille N° 117 and explanatory note. Bern.: Swisstopo, (2005).

Becker, A. , The Jura Mountains - an active foreland fold-and-thrust belt?. *Tectonophysics,* **321**, (2000), p. 381–406.

Brentini M., Impact d'une donnée géologique hétérogène dans la gestion des géo-ressources: Analyse intégrée et valorisation de la stratigraphie à travers le bassin genevois (Suisse, France). Terre & Environnement (2018), 140, 230 pp.

Charollais, J. et al., La Molasse du bassin franco-genevois et son substratum. Archives Des Sciences,. *Archives des sciences,* 60(2–3), p. 59–174.

Charollais, J. et al. (2013). Présentation d'une nouvelle carte géologique du Vuache et du Mont de Musièges.. *Archives des sciences,* (2007), **66**, pp. 1-63.

Clerc, N. , GeoMol-CH project: Interpretation and modeling report of the Geneva area, Geneva. (2016).

David, A. and Vassilvitskii, S., k-means++: The advantages of careful seeding. *Proceedings of the eighteenth annual ACM-SIAM symposium on Discrete algorithms*, Society for Industrial and Applied Mathematics, (2007).

Dubois, M. K., Bohling, G. C. and Chakrabarti, S., Comparison of four approaches to a rock facies classification problem. *Computer and Geosciences,* **33**, (2007), pp. 599-617.

Geo-Hydro environnement. Litholog Report GEo-01. Geneva, (2018).

Gorin, G., Signer, C. and Amberger, G. ,Structural configuration of the western Swiss Molasse Basin as defined by reflection seismic data. *Eclogae Geologicae Helvetiae,* 86(3), (1993), p. 693–716.

Guellec, S.,Mugnier, J.-L., Tardy, M. and Roure, F., Neogene evolution of the western Alpine foreland in the light of ECORS data and balanced cross-section. Deep Structure of the Alps,. *Deep Structure of the Alps,* **156**, (1990), p. 165–184.

Hale, D. , Dynamic warping of seismic images. *Geophysics,* **78**, (2013), p. S105–S115.

Hale, D. , Methods to compute fault images, extract fault surfaces, and estimate fault throws from 3D seismic images. *Geophysics,* **73**, (2013), pp. O33-O43.

Hall, B. ,Facies classification using machine learning. *The Leading Edge,* **35**, (2016), p. 906–909.

Hall, M. and Hall, B, Distributed collaborative prediction: Results of the machine learning contest. *The Leading Edge,* **36**, . (2017), pp. 267-269.

Haralick, R., Shanmugam and K. Dinstein, I.. Textural features for image classification. *EEE Transactions on systems, man, and cybernetics,* **3(6)**, (1973), pp. 424-433.

Homberg, C. et al.. Structural inheritance and cenozoic stress fields in the Jura fold-and-thrust belt (France). *Tectonophysics,* **357(1-4)**, (2002), p. 137–158.

Kempf, O. and Pfiffner, O. A.. Early Tertiary evolution of the North Alpine Foreland Basin of the Swiss Alps and adjoining areas. *Basin Research,* **16(4)**, (2004), pp. 549-567.

Kuhlemann, J. and Kempf, O. Post-Eocene evolution of the North Alpine Foreland Basin and its response to Alpine tectonics. *Sedimentary Geology,* **152(1-2)**, (2002), pp. 45-78.

Li, F. and Lu, W. Coherence attribute at different spectral scales. *Interpretation,* **2(1)**, (2014), pp. SA99-SA106.

Lloyd, S. P. Least squares quantization in pcm. *IEEE Transactions on Information Theory, ,* **28(2**), (1982), pp. 129-136.

Lo, H. Y, Discrete Fracture Network Modelling in the Geneva Basin (Lower Cretaceous Carbonates): Implication for Geothermal Exploration*,* MSc, Université de Genève, (2019).

Marfurt, K. J., Kirlin, R. L., Farmer, S. L. and Bahorich, M. S. 3-D seismic attributes using a semblance-based coherency algorithm. *Geophysics,* Issue **63**, (1998). , pp. 1150-1165.

Marfurt, K. J. et al, Coherency calculations in the presence of structural dip. *Geophysics,* Issue **64**, . (1999), p. 104–111.

Mazurek, M., Hurford, A. J. and Leu, W.,. Unravelling the multi-stage burial history of the Swiss Molasse Basin: Integration of apatite fission track, vitrinite reflectance and biomarker isomerisation analysis. *Basin Research,* **18(1**), (2006), pp. 27-50.

Meyer, M.,. Le Complexe récifal kimméridgien-tithonien du Jura méridional interne (France), évolution multifactorielle, stratigraphique et tectonique.. Genève: Thèse de doctorat: Univ. Genève, (2000)

Moscariello, A., Geothermal exploration in SW Switzerland. *Proceedings* European Geothermal Congress 2016 Strasbourg, France, **19-24**, (2016), 10 pp.

Moscariello, A., Clerc, N., Eruteya, O. E., Omodeo-Salé, S. and Guglielmetti, L. (2019) Complex shortening tectonic style in the undisturbed Alpine foreland: Example from the Geneva Basin (Switzerland) and implications for subsurface geo-fluid circulation. GE-RGBA Report, University of Geneva, GEG2019001,18 pp.

Moscariello A. Guglielmetti L., Omodeo-Salé S., De Haller A., Eruteya O.E., Lo H.Y., Clerc N., Makloufhi Y., Do Couto D., Ferreira De Oliveira G. Perozzi L., DeOliveira F., Quiquerez L. Nawratil De Bono C., Meyer M. Heat production and storage in Western Switzerland: advances and challenges of intense multidisciplinary geothermal exploration activities, 8 years down the road. *Proceedings* World Geothermal Congress 2020, Reykjavik, Iceland, April 26 – May 2, (2020), , 12 pp.

Pedregosa, F. et al., Scikit-learn: Machine Learning in Python. *Journal of Machine Learning Research,* **12**, (2011),. pp. 2825-2830.

Randen, T., Pedersen, S. I. and Sønneland, L. Automatic extraction of fault surfaces from three-dimensional seismic data. *71st SEG Annual International Meeting*, San Antonio, (2001)..

Rusillon, E.,. Characterisation and Rock Typing of Deep Geothermal Reservoirs in the Greater Geneva Basin. *Terre and Environnement* 141, (2018), 252p.

Signer, C. and Gorin, G. , New geological observations between the Jura and the Alps in the Geneva area, as derived from reflection seismic data. *Eclogae Geol. Helv***, 88(2)**, (1995), pp. 235-265.

Sommaruga, A. Décollement tectonics in the Jura foreland fold-and-thrust belt. *Marine and Petroleum Geology,* **16(2)**, (1999). p. 111–134.

Thorndike and R., L, Who Belongs in the Family? *Psychometrika,* **18(4)**, . (1953)., pp. 267-276.

Van Bemmel, P. P. and Pepper, R. E., Seismic signal processing method and apparatus for generating a cube of variance values. US, Patent No. 6, (2000),. 151,555.

Worsley, K., Marret, S., Neelin, P. and Evans, A. Searching scale space for activation in PET images.. *Human Brain Mapping,* **4**, (1996), pp. 74-90.

Wu, X. and Fomel, S., Automatic fault interpretation with optimal surface voting. *Geophysics,* Issue 83, ., (2018)., pp. O67-O82.

Wu, X., Liang, L., Shi, Y. and Fomel, S., . FaultSeg3D: Using synthetic data sets to train an end-to-end convolutional neural network for 3D seismic fault segmentation. *Geophysics,* Issue 84, (2019), pp. IM35-IM45.

Wu, X. and Zhu, Z, Methods to enhance seismic faults and construct fault surfaces. *Computers and Geosciences,* Issue **107**, . (2017), pp. 37-38 .